J Mater Sci (2012) 47:6095–6107
DOI 10.1007/s10853-012-6526-8

Impact of heat treatment on the mechanical properties of AISI 304L austenitic stainless steel in high-pressure hydrogen gas

Sebastian Weber · Mauro Martin · Werner Theisen

Received: 24 November 2011 / Accepted: 20 April 2012 / Published online: 8 May 2012

Abstract Hydrogen environment embrittlement of metastable austenitic stainless steels is a well-known phenomenon partially related to the formation of strain-induced martensite. In the literature, hydrogen environment embrittlement is often discussed on the basis of nominal chemical compositions only and neglects effects of metallurgical production and processing. The aim of this study is to investigate the influence of the δ-ferrite volume fraction and grain size on the mechanical properties of a standard grade 1.4307 (AISI 304L) tested in high-pressure hydrogen gas. A negligible influence was found for δ-ferrite volume fractions between 2 and 10 %. This result is explained by the dominating influence of machining-induced α-martensite on the surface of the tensile samples. In contrast, the grain size was found to have a significant effect on hydrogen environment embrittlement. In particular, grain sizes smaller than 50 μm were found to have a higher ductility. The results are discussed with respect to stacking fault energy, formation of strain-induced α-martensite, trapping of hydrogen and microsegregations. The results are of particular interest for the materials selection and development of materials for hydrogen applications.

S. Weber (✉)
Helmholtz-Zentrum Berlin für Materialien und Energie GmbH, Hahn-Meitner Platz 1, 14109 Berlin, Germany
e-mail: sebastian.weber@helmholtz-berlin.de

M. Martin · W. Theisen
Institut für Werkstoffe, Lehrstuhl Werkstofftechnik, Ruhr-Universität Bochum, 44780 Bochum, Germany

Introduction

History seems to repeat itself: as early as 1981 Brooks and West [1] pointed the burgeoning interest in structural materials for hydrogen applications as a result of new energy strategies. At that time the energy politics of US president Jimmy Carter encouraged a changeover from conventional to alternative forms of energy supply in the United States of America. This was driven by economic reasons rather than ecologic factors, as a consequence of the steep increase in the price of crude oil. The ambitious program of President Carter was cut in the early 1980s. Today, 30 years later, gaseous and liquid hydrogen are again considered to be interesting fuels for future energy supplies, both stationary and mobile. However, storage and use of hydrogen gas in mobile applications are closely associated with hydrogen environment embrittlement (HEE). This phenomenon is characterized by deterioration of the mechanical properties caused by the presence of external hydrogen gas [2, 3]. Austenitic stainless steels are often used for hydrogen applications due to their high ductility at low temperatures, low thermal conductivity, and low HEE compared to ferritic steels and nickel alloys. Austenitic stainless steels 1.4301 (AISI 304) and 1.4307 (AISI 304L) are frequently investigated in this context: on the one hand, to compare them with existing materials or new alloys, intended for use in a hydrogen environment, and on the other hand, because of their relatively low cost, which is mandatory for applications on a massive scale. The latter requirement has generated much interest in the HEE behavior of austenitic stainless steels with a reduced nickel content of less than 10 mass%. In this group of steels, lowering of the resistance against HEE by decreasing the nickel content is accompanied by a high degree of scattering of mechanical properties in hydrogen

which has been related to segregation effects [4] and the presence of strain-induced martensite [5, 6]. In this context, the formation of strain-induced α-martensite in type 304 austenitic stainless steel and its dependence on strain rate, temperature, and deformation mode are well-known and investigated [7]. The almost complete transformation of a fully austenitic, solution-annealed structure of 304 steel to α-martensite by deformation can for instance be used for grain refinement by tempering to re-transform the martensite to austenite [8]. In this way, ultra fine-grained microstructures can be obtained. The susceptibility to hydrogen embrittlement of an austenitic steel of a given chemical composition is known to be a function of production and processing [9]. Influence of heat treatment and resulting microstructure on susceptibility to hydrogen embrittlement was also reported for ferritic pipeline steels [10]. Microstructural effects arising from processing and heat treatment are often neglected; however, they are the focus of interest in this study.

The volume fraction of δ-ferrite and the grain size of a standard 1.4307 (AISI 304L) steel were varied independently to investigate their influence on hydrogen environment embrittlement. The chemical composition of the steel was kept constant. This study examines the relationship between microstructural properties and the results of tensile tests performed in air and in high-pressure hydrogen gas at ambient temperature.

Experimental

Sample preparation

Commercial semi-finished bars of austenitic stainless steel 1.4307 (AISI 304L) were provided by Deutsche Edelstahlwerke (DEW, Witten, Germany). They were produced by continuous casting with a 265 mm square cross-section, hot-rolled in several passes to bars with a final diameter of 30 mm, and quenched. Table 1 gives the chemical composition of the steel measured by optical spark emission spectrometry. To account for macroscopic segregations, only one sample was machined from the initial cross-section, taken from the center of the bar parallel to the rolling direction. This approach insures a comparable influence of segregations for each specimen. The samples were prepared by wet turning with specific machining parameters to obtain a mean surface roughness of $R_A < 0.4$ µm. The bars were machined to cylindrical tensile specimens with a gage length of 30 mm and a diameter of 5 mm. Heat treatments were performed in a muffle-type furnace or in an industrial vacuum heat-treatment furnace equipped with a graphite heater. The specimens were quenched either in water (muffle-type furnace) or in argon gas at a pressure of 200 kPa (vacuum furnace). Cooling rates from the solution-annealing temperature were sufficiently high to insure a fully austenitic microstructure free of precipitated carbides. Some of the samples were ground and polished to remove the mechanically deformed surface layer arising from machining. About 100 µm of the radius in the gage section of as-machined samples were removed by manual grinding with moistened silicon carbide abrasive paper. Silicon carbide mesh sizes of 320, 500, 800, and 1000 were used sequently followed by a manual polishing with diamond suspension impregnated pieces of cotton batting. For polishing, diamond suspensions with grain sizes of 6, 3, 1, and 0.25 µm were used sequently finally leading to a mirror polish gage section free of scratches. The removal of martensite was checked metallografically in comparison to as-machined samples and no indication for this structure found. However, the presence of an ultra-thin surface layer of martensite after manual grinding and polishing that is not visible in metallographic inspection cannot be ruled out.

Microstructure

For microstructural investigations, longitudinal and transverse cross-sections were prepared metallographically by cutting and embedding the samples followed by grinding and polishing according to standard preparation routes. Samples for measuring the grain size using image analysis were etched with V2A solution (100 ml H_2O, 100 ml HCl, 10 ml HNO_3). Grain size was determined by linear intercept method without considering the twin grain boundaries. Sample for quantification of δ-ferrite using image analysis were etched with Beraha II (67 ml H_2O, 33 ml HCl, 4 g $(NH_4)HF_2$, 1 g $K_2S_2O_5$). The amount of ferrite in the unstrained state was additionally determined using a FeritScope® MP30 device (Helmut Fischer GmbH, Sindelfingen, Germany). The same device was also used to measure the formation of α-martensite during tensile straining in air. In accordance with the literature, the

Table 1 Bulk chemical composition of the investigated austenitic stainless steel; values in mass % with iron being the dependent substitutional element

	C	Si	Mn	P	S	Cr	Ni	Mo	Cu	V	Co	N
1.4307	0.016	0.68	1.95	0.03	0.026	17.89	8.63	0.29	0.59	0.09	0.10	0.071

Feritscope® readings were multiplied by a factor of 1.7 to obtain the mass fraction of α-martensite [11]. Microstructure was investigated by light optical microscopy with an Olympus BX-60M microscope. Fracture surfaces were investigated with a Keyence VHX600 optical microscope and a JEOL JSM840 scanning electron microscope.

Tensile tests

Tensile tests were performed in air at room temperature and ambient pressure and in pure hydrogen gas (≥99.9999 % H_2) at a pressure of 40 MPa and 25 ± 3 °C. Tensile tests in hydrogen were performed by The Welding Institute (TWI, Cambridge, UK). The initial strain rate of all tensile tests was 5.5×10^{-5} s^{-1} which was comparable to the value used by Zhang et al. [12] and is in agreement with ASTM standard G142-98 for testing of metals in hydrogen [13]. In addition to determining the yield strength, tensile strength and elongation at fracture, the relative reduction of area was measured ex-situ with a caliper, because this quantity is known to be a sensitive measure for hydrogen embrittlement [14, 15].

Results

Material

In the as-received condition, the bar material of 1.4307 exhibited a mean grain size of 13 µm and contained 3.5 vol% δ-ferrite. The grain size and δ-ferrite content were independently adjusted by means of appropriate heat treatments. The aim was to obtain two different sets of sample conditions:

1. "Industrial condition" with measurable amounts of δ-ferrite and machining-induced α-martensite on the surfaces as a result of turning and milling.
2. "Scientific condition" without δ-ferrite and without machining-induced α-martensite.

The heat treatments were planned by calculating a carbon isopleth for the alloy composition given in Table 1 using the Calphad software ThermoCalc S [16] and the TCFe6.2 thermodynamic database [17]. Results of the equilibrium calculation are depicted in Fig. 1. The standard solution-annealing temperature of 1050 °C is indicated by a white circle. The appropriate temperature intervals for adjusting the amount of δ-ferrite and changing the grain size are also shown. It is important to note that short-term annealing in the phase field of γ and δ results in fast formation of δ-ferrite without significant differences in grain size. The evolution of the equilibrium volume fraction of δ-ferrite, also calculated with Calphad, is shown in Fig. 2.

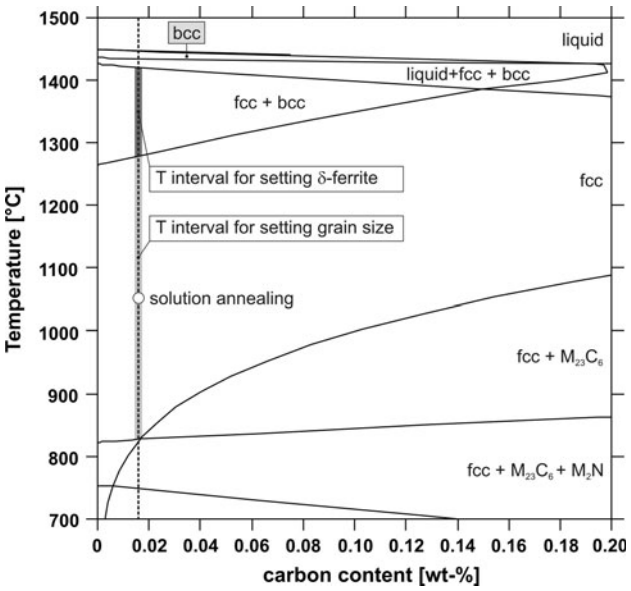

Fig. 1 Calculated phase diagram of austenitic stainless steel 1.4307 (AISI 304L) with the chemical composition given in Table 1

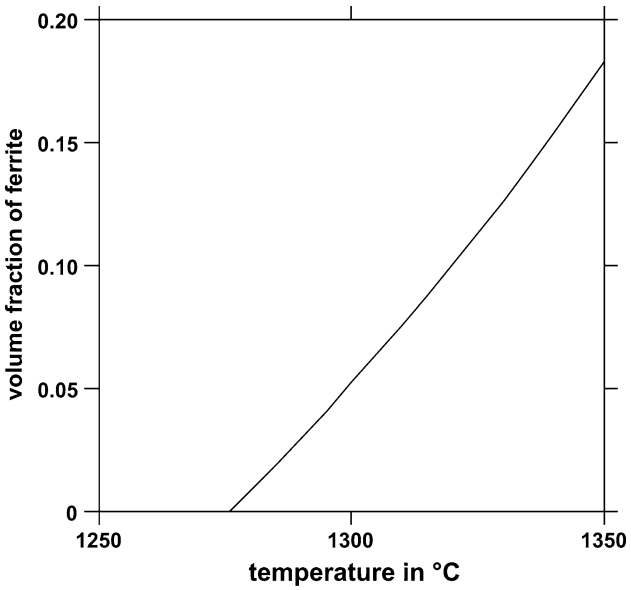

Fig. 2 Calculated equilibrium volume fraction of δ-ferrite in 1.4307 (AISI 304L) as a function of the temperature

Three different temperatures were chosen, namely 1300, 1320, and 1340 °C, which led to δ-ferrite volume fractions of 2, 6, and 10 vol%. For these heat treatments, a constant dwell time of 5 min at the heat treatment temperature resulted in a grain size of 60–65 µm in all samples. Annealing at a lower temperature in the γ phase field changed the grain size and reduced the δ-ferrite content to less than 0.1 vol% at the same time. Annealing at temperatures of 1050 or 1200 °C led to a characteristic change in grain size, as shown in Fig. 3. Changing the heat

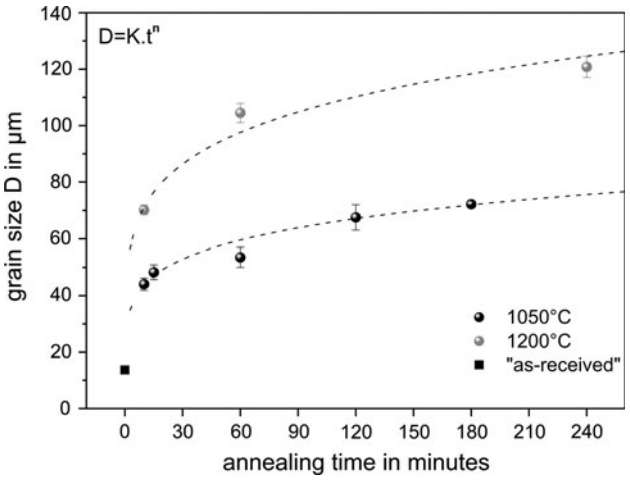

Fig. 3 Grain size in 1.4307 (AISI 304L) as a function of temperature and time

treatment temperature and dwell time produced mean grain sizes of 50, 70, 110, and 130 µm. In addition, the material in the as-received state with a grain size of 13 µm was tested without an additional heat treatment. Optical micrographs exemplify two different grain sizes and two different volume fractions of δ-ferrite (Fig. 4).

Table 2 Mechanical properties of samples of 1.4307 with different contents of δ-ferrite determined by tensile testing at 25 °C in air ($p = 0.1$ MPa) and in a hydrogen atmosphere ($p = 40$ MPa)

δ-Ferrite (vol%)	Atmosphere	$R_{p0.2}$ (MPa)	R_m (MPa)	A (%)	Z (%)
2	Air	227	637	75	82
2	H_2	233	544	37	25
6	Air	232	631	71	82
6	H_2	236	549	37	26
10	Air	240	634	65	81
10	H_2	252	558	34	25

$R_{p0.2} = 0.2$ % offset yield strength, R_m tensile strength, A elongation at fracture, Z reduction of area

Tensile tests

Results of tensile testing in air and hydrogen are given in Table 2 for samples with differing volume fractions of δ-ferrite. The yield strength was slightly affected, showing increasing values with increasing amount of δ-ferrite. There was no significant difference in the yield strength determined in air and hydrogen. In contrast, the tensile strength of samples tested in gaseous hydrogen was lower for all three conditions. Important measures of ductility are

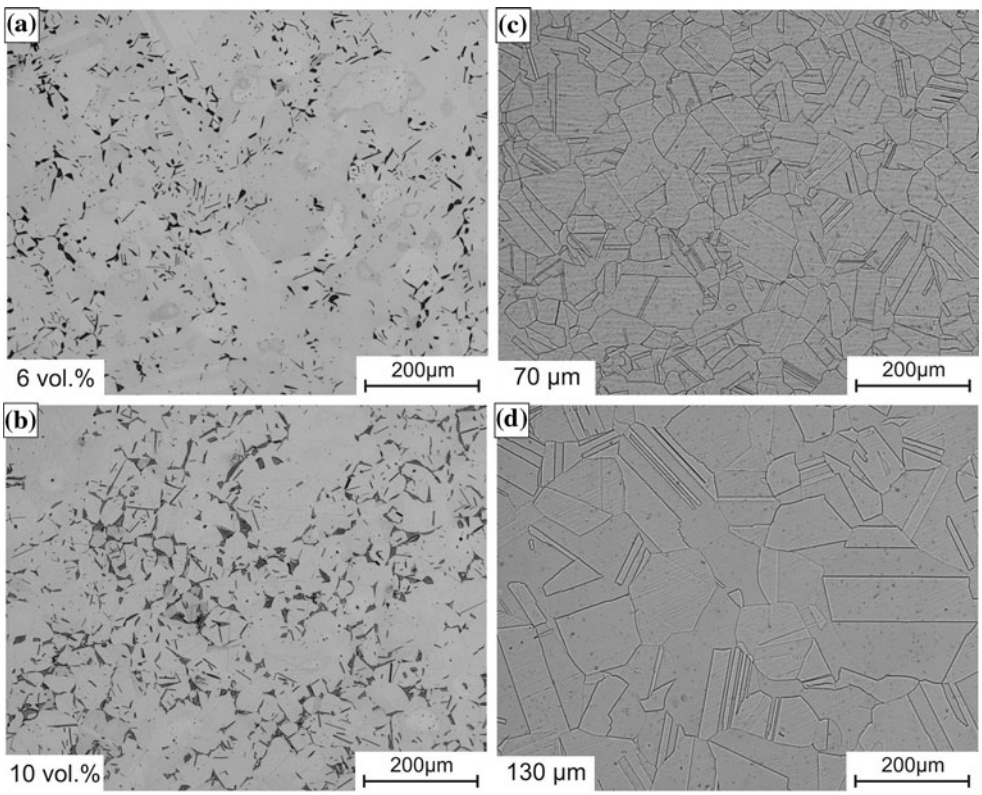

Fig. 4 Optical micrographs of 1.4307 (AISI 304L) with different grain size and different volume fractions of δ-ferrite. *Dark* microstructural features in **a** and **b** show δ-ferrite

Table 3 Mechanical properties of samples of 1.4307 with different grain size determined by tensile testing at 25 °C in air ($p = 0.1$ MPa) and in a hydrogen atmosphere ($p = 40$ MPa)

Grain size (μm)	Atmosphere	$R_{p0.2}$ (MPa)	R_m (MPa)	A (%)	Z (%)
13 (polished)	Air	278	638	60	83
13 (polished)	H_2	275	634	54	63
50	Air	212	655	75	81
50	H_2	191	605	58	40
70	Air	203	641	80	82
70	H_2	206	598	57	34
110	Air	205	626	80	82
110	H_2	201	597	58	35
130	Air	202	616	78	82
130	H_2	202	580	53	33
130 (polished)	Air	184	607	68	82
130 (polished)	H_2	174	588	54	50

$R_{p0.2}$ = 0.2 % offset yield strength, R_m tensile strength, A elongation at fracture, Z reduction of area

elongation at fracture (A) and reduction of area (Z). A comparison of these parameters determined in air and hydrogen clearly shows significant embrittlement by gaseous hydrogen. Higher volume fractions of δ-ferrite led to a reduced elongation at fracture for the samples tested in air. However, the influence of testing in hydrogen was similar for all three conditions, and no dependence of hydrogen environment embrittlement on volume fraction of δ-ferrite was found.

The results for different grain sizes are given in Table 3. The samples in the as-received condition had the highest yield strength due to their smallest grain size and a δ-ferrite volume fraction of 3.5 %. All other samples exhibited similar yield strengths, irrespective of the testing condition. The tensile strength was lower for samples tested in hydrogen; however, the influence was less pronounced compared to samples with varying δ-ferrite content. Finally, hydrogen environment embrittlement was found to be dependent on the grain size. Samples with a smaller grain size showed higher values of elongation at fracture and reduction of area compared to samples with a coarse-grained microstructure. A grain size exceeding 70 μm did not seem to have a further effect on the ductility in hydrogen. A comparison of the results of unpolished and polished samples with a grain size of 130 μm showed that polishing had a positive effect. However, a comparison of the Z values of polished samples with 13 and 130 μm grain size showed that the gain in ductility was dominated by small grain sizes. Exemplary stress–strain curves of polished samples with mean grain sizes of 13 μm and 130 μm are depicted in Fig. 5. The flow stresses of the samples with a mean grain size of 13 μm are almost equal independent of the atmosphere. Offset yield strength is higher compared to the coarse-grained steel. For the latter, lower flow stresses are measured by testing in hydrogen. Furthermore, serrations in the stress–strain curve of the material with a mean grain size of 130 μm occur during testing in hydrogen. These serrations are not visible to such an extent in the curves of the fine-grained samples. The influence of grain size on HEE was visualized by calculating the relative values of the mechanical properties such as relative reduction of area:

$$\text{rel.}Z = \frac{Z(H_2)}{Z(\text{air})} \times 100 \quad (1)$$

The results are depicted in Fig. 6. Values close to 100 % indicate a complete resistance to embrittlement. The positive influence of the smaller grain size is clearly visible for both parameters, relative A and relative Z.

Fractography

Figure 7 shows optical micrographs of the surfaces of tensile specimens after testing in hydrogen. A comparison of the two sets of samples with varying δ-ferrite content or grain size reveals a significant difference. All samples containing δ-ferrite exhibited numerous large circumferential secondary cracks. These secondary cracks are also found on the surfaces of tensile samples with varying grain size; however, their size is remarkably smaller. Figure 8 shows optical microscopy images of the fracture surfaces of samples with 13 and 130 μm grain size. The greater necking of the large-grained sample is clearly visible (Fig. 8a, c). A comparison of Fig. 8b, d reveals differences in the surface roughness. The surface of the fine-grained

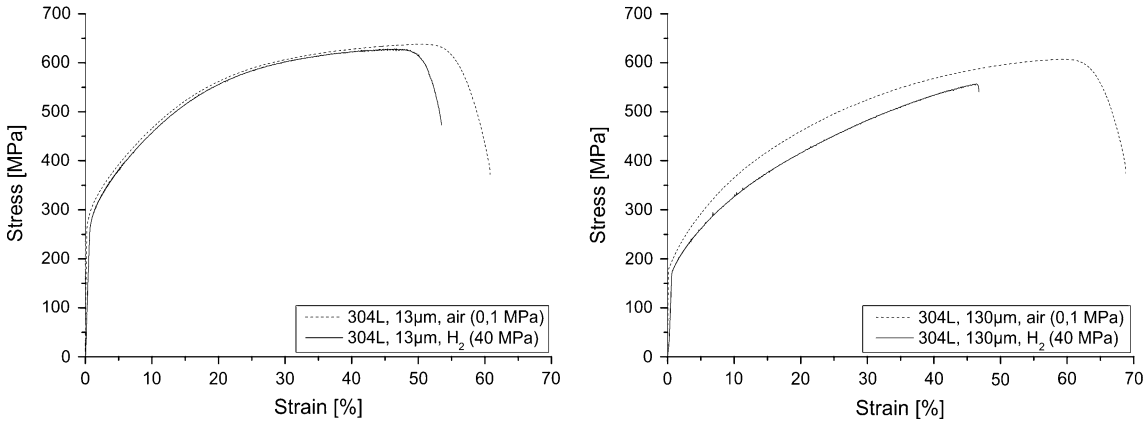

Fig. 5 Stress–strain curves of polished samples with mean grain sizes of 13 and 130 µm in air (0.1 MPa) and gaseous hydrogen (40 MPa)

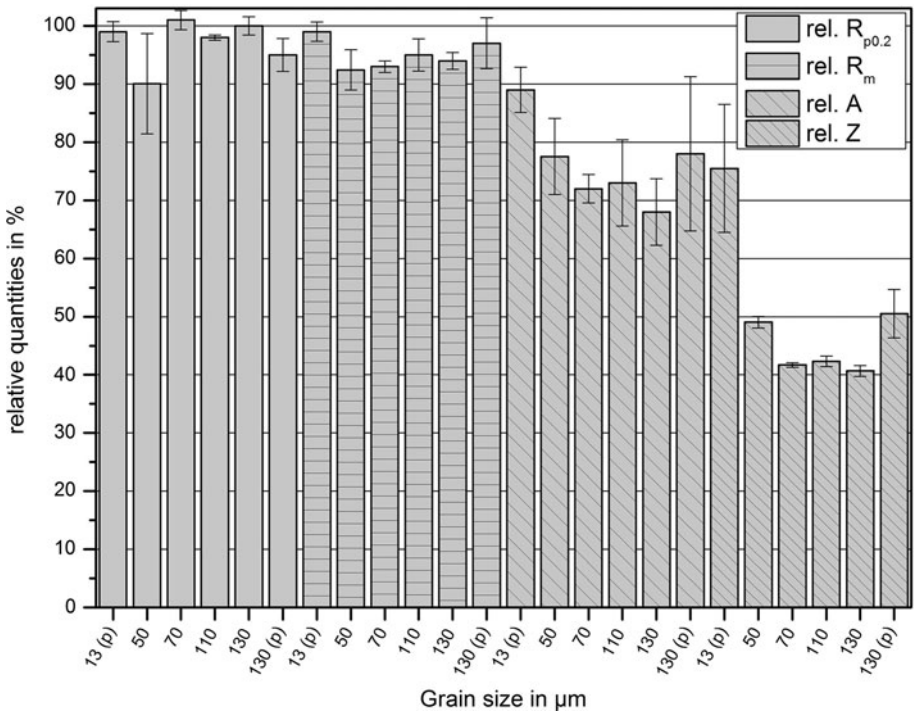

Fig. 6 Relative mechanical properties obtained by tensile testing in air (0.1 MPa) and gaseous hydrogen (40 MPa). Samples with polished surfaces prior to testing are indicated by (*p*)

material shows a lower surface roughness. Detailed fractographic images taken by scanning electron microscopy are shown in Fig. 10. The coarse-grained material (Fig. 10d–f) reveals evidence of a fully brittle failure characterized by a transgranular and cleavage-like fracture. A comparison with the fine-grained material (Fig. 10a–c) reveals significant differences. Besides greater necking, this material shows partially ductile fracture. About one third of the fracture surface, indicated by a 'D' in Fig. 10a, shows ductile fracture and dimples. The remaining part of the fracture surface, indicated by a 'B' in Fig. 10a, shows brittle fracture. A comparison of Fig. 10b, f does not show significant differences. Both fractographic images are typical for hydrogen-assisted fracture of austenitic steels.

Discussion

Influence of δ-ferrite

Independent of the aspect of hydrogen embrittlement, δ-ferrite has a measurable effect on the yield strength of the metastable austenitic stainless steel tested in this study. Islands of δ-ferrite (Fig. 4) act as particulate reinforcements and increase the strength of the material with increasing volume fraction. Accordingly, elongation at fracture is reduced with increasing δ-ferrite content. Owing to the fact that δ-ferrite is preferentially found at the triple points and along austenite grain boundaries, it can be expected to influence the mechanical properties in hydrogen, because

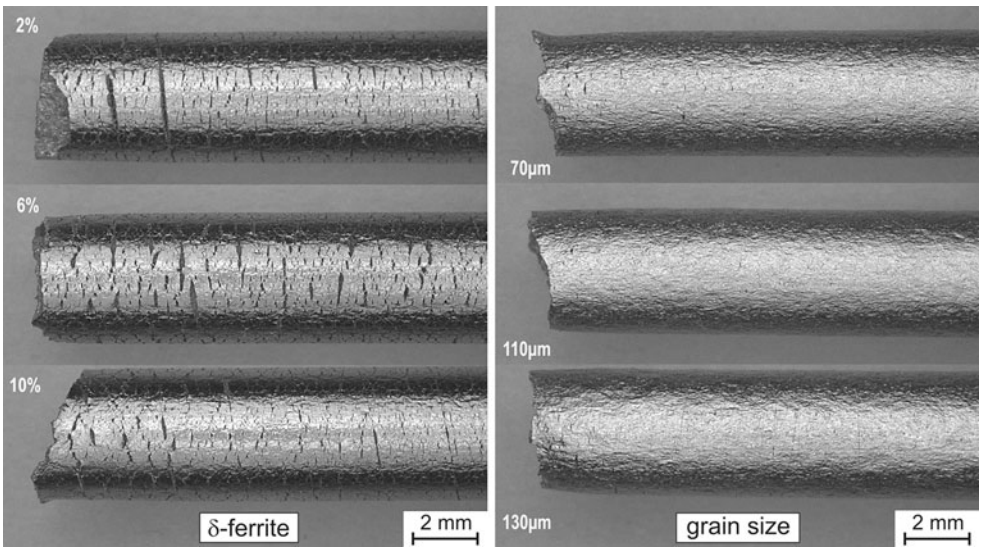

Fig. 7 Optical micrographs of the surface of samples after tensile testing in hydrogen (40 MPa) at 25 °C. *Left* variation of δ-ferrite. *Right* variation of grain size

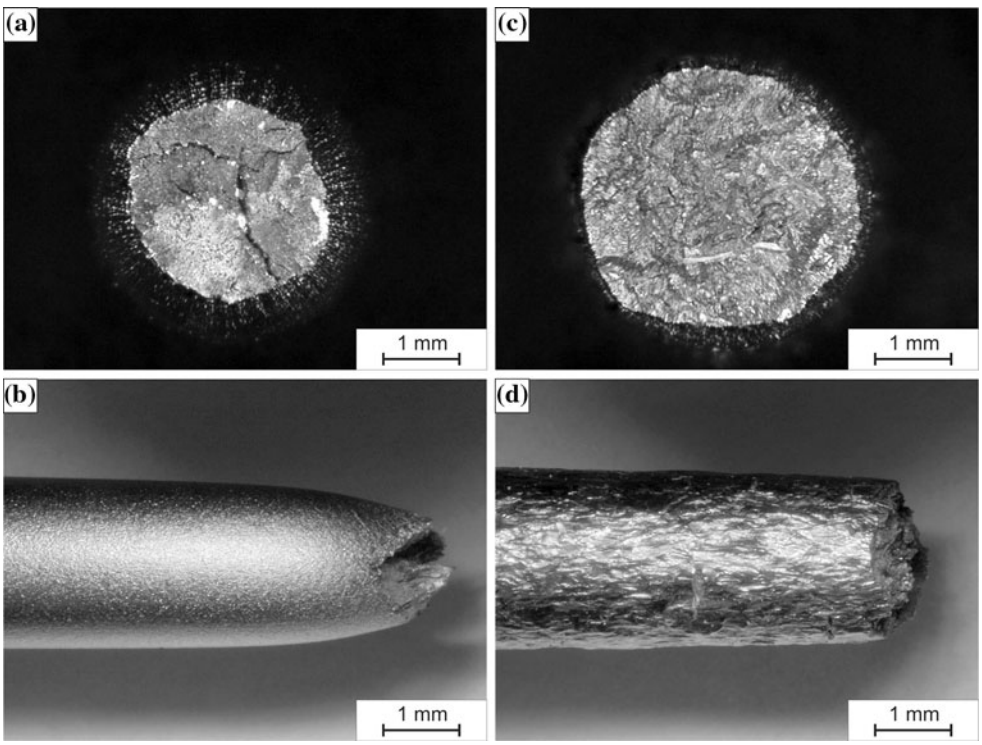

Fig. 8 Optical microscopy fractographic images of 1.4307 (AISI 304L) after tensile testing in hydrogen. **a**, **b** The material with a grain size of 13 µm. **c**, **d** The material with 130 µm. Both samples had a polished surface finishing prior to tensile testing

diffusion of hydrogen in ferritic structures is faster than in austenite [5, 18]. Furthermore, account must be taken of the fact that the tests performed here are evaluating hydrogen environment embrittlement, which implies no pre-charging of the samples prior to testing in gaseous hydrogen. Therefore, interaction of the steel with gaseous hydrogen is of importance for the mechanical properties of the material. This study did not reveal evidence of the expected ductility loss due to δ-ferrite. Considering only the reduction of area as a sensitive measure for hydrogen embrittlement [14, 15], no influence of δ-ferrite was found at all. This can be explained by the formation of strain-induced α-martensite on the surface of the tensile samples during machining. For this study, the bar material was heat treated prior to

machining in a muffle-type furnace to obtain a pre-defined amount of δ-ferrite. Samples were subsequently machined to the final dimensions to reproduce industrial production of parts. However, a thin layer (50–100 μm) of α-martensite on the surface cannot be avoided, as it could be shown by the same authors in a former work [18]. An additional solution annealing heat treatment to remove α-martensite was excluded because it would have altered the δ-ferrite content and is not common practice in industrial applications. During tensile testing in hydrogen, the superficial α-martensite is easily saturated with hydrogen due to its high diffusivity in α-Fe. Hydrogen is absorbed from the gas phase after the thin passivation on the steel surface layer is damaged. The surface layer of α-martensite is embrittled by the dissolution of hydrogen resulting in the formation of circumferential cracks perpendicular to the direction of load (Fig. 7). Stress concentration at the crack tips leads to localized accumulation of hydrogen and brittle failure. Furthermore, the α-martensite present at the surface can act as a nucleation site for additional α-martensite and hydrogen embrittlement [18–20]. The results of the tensile tests on samples with different amounts of δ-ferrite can easily be interpreted on the basis of this information: the presence of α-martensite on the surface of the samples dominates the mechanical properties obtained in hydrogen and does not allow differentiation according to differing δ-ferrite contents. In addition, the volume fraction of δ-ferrite investigated in this study is comparatively low. Literature data confirms that no significant loss of ductility in hydrogen can be expected for up to 10 vol% δ-ferrite [1, 21]. Higher volume fractions of δ-ferrite in relation to hydrogen embrittlement of AISI-type 304L steel were investigated by Buckley and Hardie. They found a slight decrease in the ductility response in hydrogen with respect to reduction of area for δ-ferrite volume fractions of up to 35 %. However, the presence of δ-ferrite is not essential for embrittlement nor is it the dominating factor [22]. In can thus be stated that HEE of 304L tested in an "'industrial"', as-machined condition arises from the machining-induced α-martensite at the surface and no additional degradation of mechanical properties by δ-ferrite up to 10 vol% occurs. Thus, certain amounts of δ-ferrite can be accepted to improve weldability but α-martensite should be removed or avoided during production [18].

Influence of grain size

To adjust the grain size, the bar material in the as-received condition was heat treated in a muffle-type furnace, water quenched, machined into tensile samples and finally solution annealed for 30 min at 1050 °C in a vacuum. The last step was applied to remove superficial α-martensite formed during turning. The solution annealing treatment was performed at lower temperature than the first heat treatment that adjusted the grain size, and this second treatment did not affect the grain size. This procedure was used to produce samples with four different mean grain sizes of 50, 70, 110, and 130 μm. In addition, a fifth grain size was obtained by using the as-received material. Samples in the as-received condition were turned from bar material to their final dimensions and manually polished to remove superficial α-martensite. These samples contained 3.5 vol% δ-ferrite, and all other samples contained less than 0.1 vol%. To rule out the sole influence of surface polishing, additional samples with a grain size of 130 μm were manually polished after turning. This experimental approach implies that the results of tensile testing should primarily reflect the influence of grain size on hydrogen environment embrittlement. Clear evidence for a positive effect of a small grain size was reported by Rozenak and Eliezer [9], who investigated the grain size dependence of hydrogen embrittlement of AISI 316, 321 and 347 austenitic steel. These authors found increasing ductility in terms of elongation at fracture with decreasing grain size. "A significant feature of the results is that decreasing the prior austenite grain size increases the mechanical properties and the resistance of AISI-type 316, 321 and 347 steels to hydrogen embrittlement."[9]. However, a well-founded explanation for this result is not provided. The effect of grain size is not easy to describe because several microstructural properties are dependent upon it. The following effects shall be considered in the discussion of the current results:

1. The influence of grain size on the effective diffusivity of hydrogen in the austenitic structure.
2. The influence of grain size on the stacking fault energy and thus on the tendency of the austenitic lattice to transform into α-martensite during deformation.
3. The rate of hydrogen absorption from the gaseous state depending on the grain size.
4. The change of chemical homogeneity during heat treatment.

Diffusivity

Typically, diffusion along grain boundaries is several orders of magnitude faster than bulk diffusion due to a lower atomic density. Recent investigations on grain size dependence of effective hydrogen diffusion coefficients in austenitic steel performed by Mine et al. showed that diffusion is enhanced by small grain sizes. This effect is explained by short-circuit diffusion along grain boundaries due to a high activation energy for the diffusion of hydrogen in bulk austenitic steels [23]. In addition, high-pressure torsion and subsequent annealing is shown in the same work to increase the density of trapping sites for

hydrogen. The higher density of traps does not originate from a smaller grain size but a higher dislocation density [23]. Grain boundaries were shown to contribute to hydrogen trapping to a neglectable extent in austenitic stainless steel [24]. Because the effective diffusivity of hydrogen increases with decreasing grain size, it cannot serve as an explanation for the experimental results obtained in this study. The smaller grain size does not retard but enhances the movement of hydrogen atoms from the gas–metal interface to the interior. Therefore, a more distinct hydrogen environment embrittlement should occur for fine-grained samples which is not the case for the results presented here.

Strain-induced α-martensite

A reason for the reduced hydrogen environment embrittlement of samples with a small grain size could be the influence on the stacking fault energy. Jun and Choi [25] showed that a reduction in grain size leads to an increase in the stacking fault energy. The latter quantity is directly related to the propensity of metastable austenitic steels to undergo strain-induced transformation to martensite. Varma et al. investigated the formation of deformation-induced martensite of AISI 304 and 316 steels. Under uniaxial straining at room temperature they found no pronounced deformation-induced transformation in AISI 316, whereas measurable amounts of α-martensite were formed in AISI 304. The amount of α-martensite was shown to decrease with decreasing grain size in the range from 53 to 285 μm [26]. These results are consistent with the findings of Nohara et al. [27]. But how does the formation of α-martensite influence the mechanical properties obtained in gaseous hydrogen? The reason is the difference in diffusivity of hydrogen in the γ and α lattices. The latter exhibits a hydrogen diffusivity that is several orders of magnitude higher compared to the austenitic structure. Therefore, the formation of α-martensite enhances hydrogen penetration throughout the volume of the sample [18]. Furthermore, formation of α-martensite leads to local stress concentration and, depending on testing temperature, fast accumulation of hydrogen atoms in the related stress fields.

To prove the theory that the grain size influences the formation of strain-induced α-martensite, additional tensile tests were performed with in-situ measurements using magnetic methods. Two sets of samples with a mean grain size of 13 (as-delivered) and 130 μm (heat-treated) were subjected to uniaxial tensile testing at room temperature in air with an initial strain rate of $5.5 \times 10^{-5}\ s^{-1}$. The FeritScope® device was used to measure the volume fraction of ferrite in the initial state and during tensile testing. α-martensite was quantified by multiplying the readings by a factor of 1.7 [11]. The δ-ferrite content

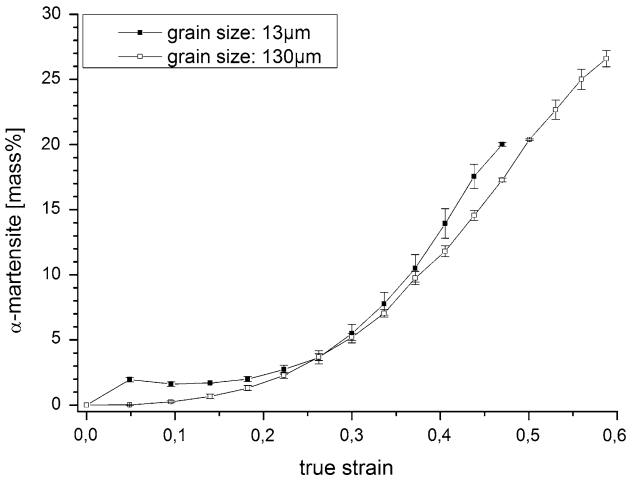

Fig. 9 Influence of grain size on the formation of strain-induced martensite in 1.4307 (AISI 304L) steel during tensile testing at room temperature

present in the unstrained condition was then subtracted. The results are plotted in Fig. 9 as mean values of α-martensite mass fraction against true strain. The amount of α-martensite in the samples with a small grain size is slightly higher throughout the whole tensile test, even though the same strain rate was applied implying that strain rate dependence of the deformation mechanism can be ruled out. The coarse-grained samples do not form strain-induced martensite at a true strain of 5 % which is in agreement with results of Kundu and Chakraborti [7] who reported only planar slip in 304 steel for low strain values and low strain rate. At high strain values, both materials reach a saturation level. The results of the measurements are in contrast to those obtained by Varma et al. [26]. Furthermore, they do not support the theory that a larger amount of strain-induced α-martensite in the coarse-grained material is responsible for its inferior performance in hydrogen gas.

Absorption of hydrogen

The difference in mechanical properties must have another reason than hydrogen diffusivity and formation of strain-induced martensite. Fractographic pictures of samples tested in hydrogen give a first hint (Fig. 8). A comparison of Fig. 8b, d reveals visible differences in the surface condition after tensile testing. The fine-grained material retains a comparatively smooth surface with low roughness. In contrast, the coarse-grained material shows a significantly higher surface roughness. This influence of grain size on the surface roughness of austenitic steel after plastic deformation was also reported by Ulvan and Koursaris [28]. It is worth mentioning in this context that the surface of both samples shown in Fig. 8 was polished to a mirror finish before tensile testing. A prerequisite for hydrogen

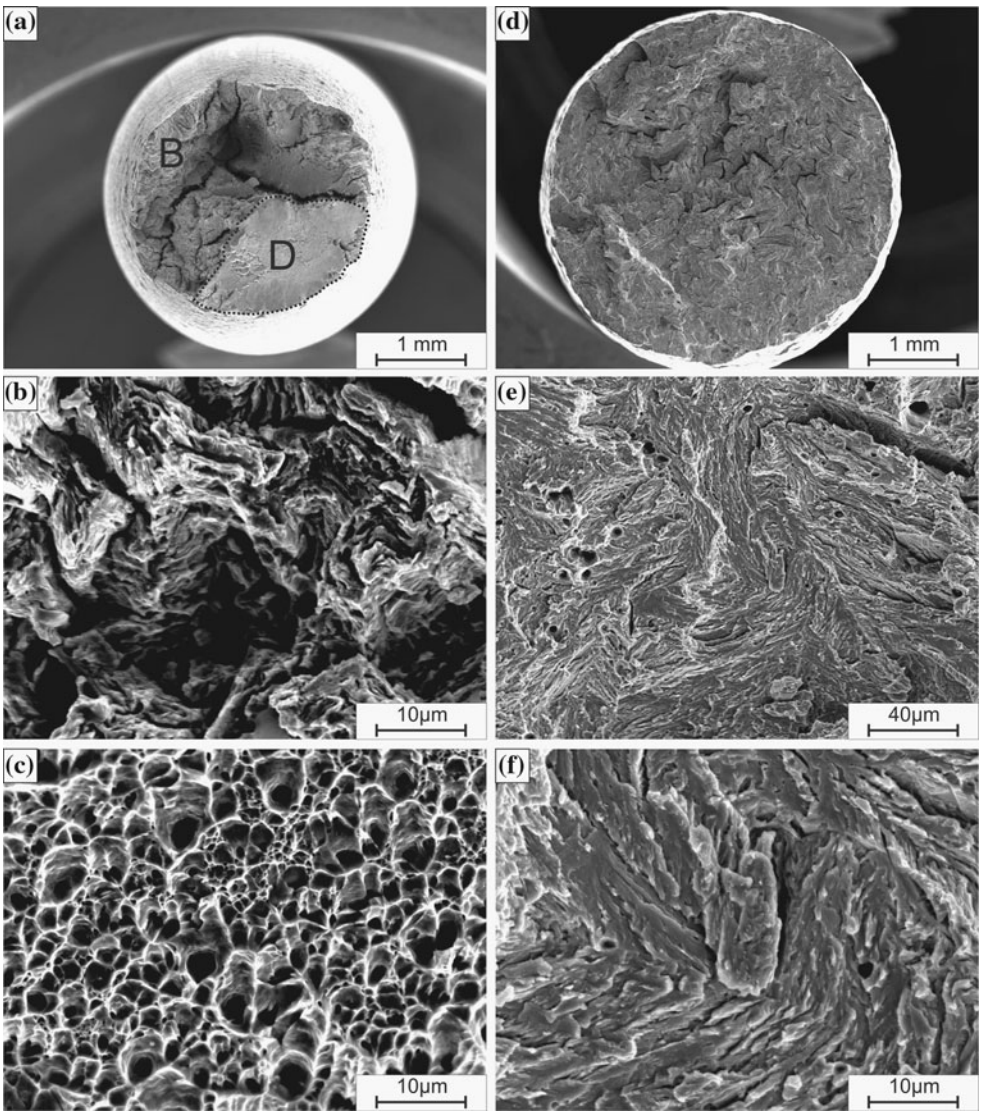

Fig. 10 SEM fractographic images of 1.4307 (AISI 304L) after tensile testing in hydrogen. **a–c** The material with a grain size of 13 µm. **d–f** The material with 130 µm. Region '*B*' in **a** shows brittle fracture, region '*D*' shows ductile fracture

environment embrittlement is the adsorption and dissociation of molecular hydrogen on the surface [29, 30]. The latter step, dissociation, is effectively hindered by the natural passivation layer that immediately forms under ambient conditions. This passivation layer has to be destroyed locally to give a fresh metal surface that allows dissociation and uptake of atomic hydrogen. In case of a quick re-passivation by a sufficient oxygen partial pressure, hydrogen environment embrittlement is reduced [31]. The authors propose that a rough surface with numerous protrusions provides more sites for hydrogen entry and a higher local stress concentration compared to the comparatively smooth surface of the fine-grained material, both effects promoting hydrogen environment embrittlement. This theory is supported by the larger number and greater length of secondary cracks in the lateral area of the coarse-grained material. Longitudinal cross-sections of samples after tensile testing in hydrogen show transgranular secondary cracks running almost perpendicular from the surface into the material (Fig. 11). Short cracks found in the fine-grained material, such as that depicted in Fig. 11a, can be stopped by grain boundaries. This effect is not found in the coarse-grained material (Fig. 11b).

Chemical homogeneity

A last aspect that should not be ignored is the influence of heat treatment on the microstructure of the material with respect to chemical homogeneity. In the as-delivered and fine-grained condition, the austenitic steel not only contains a few percent of δ-ferrite, but it also exhibits significant microsegregations. The segregation bands are elongated in

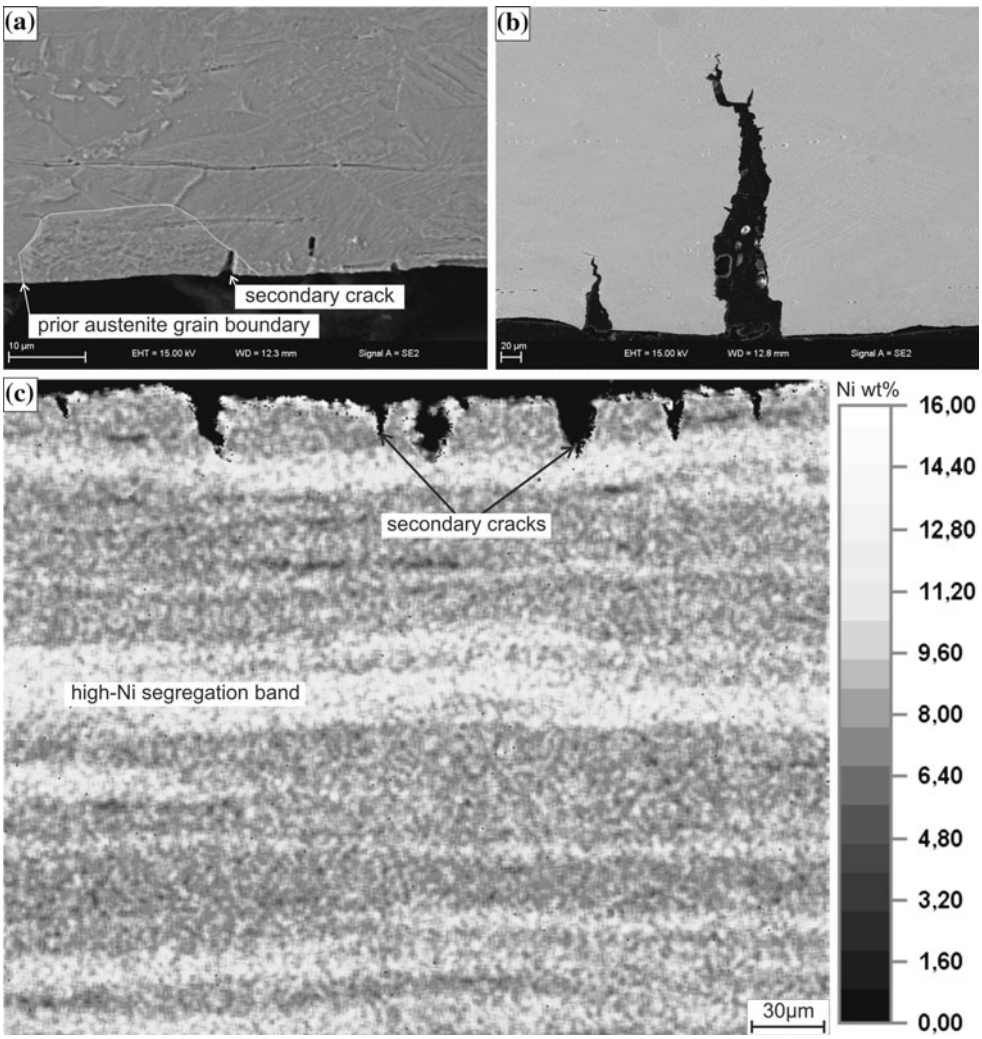

Fig. 11 Micrographs of metallographic cross-sections of tensile samples (1.4307 (AISI 304L)) after tensile testing in hydrogen showing secondary cracks formed at the surface. **a** The material with a grain size of 13µm. **b** The material with 130µm. **c** Secondary cracks stopped by segregation bands with a high-nickel content in a sample with a grain size of 50 µm

the forging direction and can be easily detected as areas with a high density of shear bands and strain-induced martensite after tensile testing (Fig. 12a, b). In previous investigations the greater stability of these areas against strain-induced transformation could be related to higher levels of almost all alloying elements, especially nickel [32, 33]. The highly alloyed segregated bands are able to stop hydrogen-assisted cracks running perpendicular to them, as shown in Fig. 11c. However, they were almost totally eliminated by heat treatment at 1200 °C for 4 h which produced a mean grain size of 130 µm (Fig. 12c, d). For this reason, crack propagation is not hindered by highly alloyed microsegregated bands in the coarse-grained samples, even though this effect has nothing to do with the grain size.

Conclusions

Modification of just one microstructural feature of a standard austenitic stainless steel turned out to be more or less impossible in this study. The following conclusions can be drawn from the results:

- δ-Ferrite volume fractions of up to 10 % do not have an additional negative effect on hydrogen environment embrittlement. The α-martensite layer present on technical surfaces of 304L dominated HEE.
- Higher ductility of a metastable austenitic steel in hydrogen for a given chemical composition and grain size necessitates the removal of α-martensite at the surface.
- A higher amount of α-martensite was not found in samples with a grain size of 130 µm compared to samples with a grain size of 13 µm. Formation of strain-induced α-martensite thus cannot serve as explanation for lower HEE of fine-grained samples.
- Large grains promote the formation of a rough surface during plastic deformation, enhance destruction of the passivation layer, and thus promote the absorption of hydrogen from the gas phase.

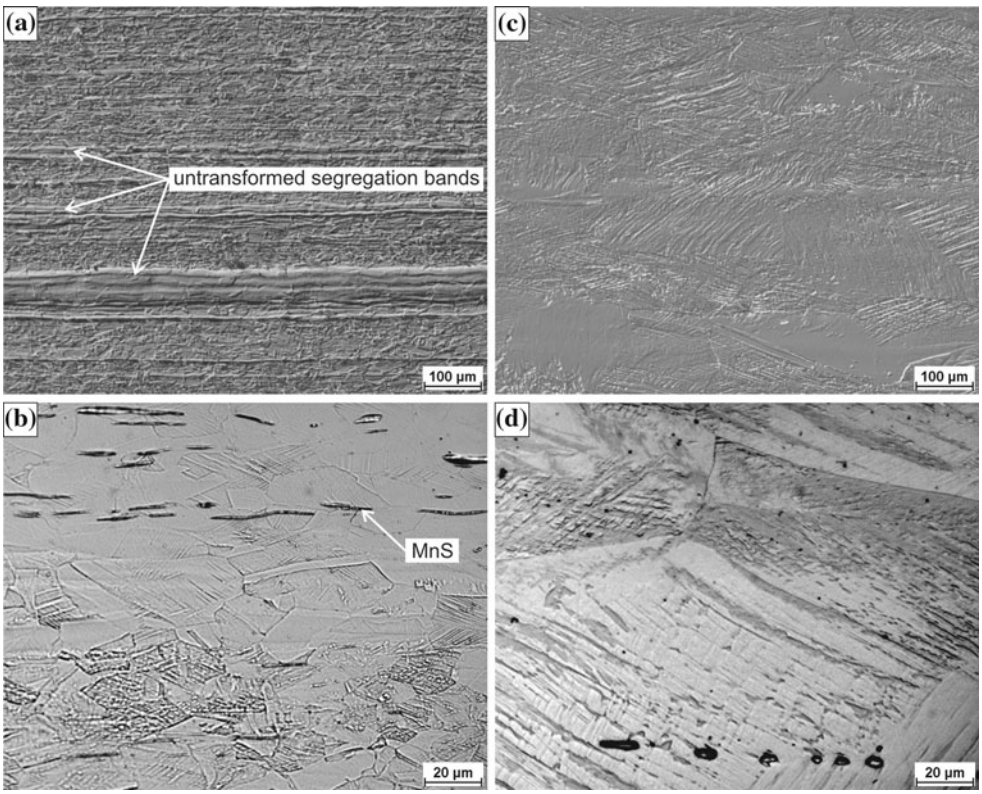

Fig. 12 Light optical micrographs of longitudinal metallographic sections of 1.4307 (AISI 304L) after tensile testing in hydrogen. **a**, **b** The material with a grain size of 13 µm; **c**, **d** the material with 130 µm

- Growth of small hydrogen-assisted cracks can be stopped by obstacles such as grain boundaries.
- Any heat treatment that enables diffusion of substitutional elements decreases the degree of segregation and, at least for metastable austenitic steels with respect to formation of α-martensite, increases hydrogen environment embrittlement.

Acknowledgements The authors gratefully acknowledge financial support from the Bundesministerium für Wirtschaft und Technologie (BMWi) under contract number 0327802D. Tensile tests in hydrogen were performed at 'The Welding Institute' (TWI, Cambridge, UK).

References

1. Brooks JA, West AJ (1981) Metall Trans A Phys Metall Mater Sci 12(2):213
2. Borchers C, Michler T, Pundt A (2008) Adv Eng Mater 10(1–2):11
3. Marchi CS, Somerday BP, Robinson SL (2007) Int J Hydrogen Energy 32(1):100
4. Michler T, Lee Y, Gangloff RP, Naumann J (2009) Int J Hydrogen Energy 34(7):3201
5. Perng TP, Altstetter CJ (1986) Acta Metall 34(9):1771
6. Perng TP, Altstetter CJ (1987) Metall Mater Trans A-Phys Metall Mater Sci 18(1):123
7. Kundu A, Chakraborti PC (2010) J Mater Sci 45:5482. doi:10.1007/s10853-010-4605-2
8. Kumar BR, Das SK, Mahato B, Ghosh RN (2010) J Mater Sci 45:911. doi:10.1007/s10853-009-4020-8
9. Rozenak P, Eliezer D (1983) Mater Sci Eng 61:31
10. Huang F, Li XG, Liu J, Qu YM, Jia J, Du CW (2011) J Mater Sci 46:715. doi:10.1007/s10853-010-4799-3
11. Talonen J, Aspegren P, Hanninen H (2004) Mater Sci Technol 20(12):1506
12. Zhang L, Wen M, Imade M, Fukuyama S, Yokogawa K (2008) Acta Mater 56(14):3414
13. G142-98(2004) (2004) In: Standard test method for determination of susceptibility of metals to embrittlement in hydrogen containing environments at high pressure, high temperature, or both. ASTM International, West Conshohocken. doi:10.1520/G0142-98R04
14. Louthan MR, Caskey GR, Donovan JA, Rawl DE (1972) Mater Sci Eng 10(6):357–368
15. Han G, He J, Fukuyama S (1998) Acta Mater 46(13):4559
16. Thermo-Calc Software AB (2010) In: Thermo-calc user's guide version S, Foundation of Computational Thermodynamics, Stockholm
17. Sundmann B, Shi P, Bratberg J (2008) In: TCFE6: TCS steels/Fe-alloys database version 6 (Juni 2008), Thermo-Calc Software AB, Stockholm
18. Martin M, Weber S, Izawa C, Wagner S, Pundt A, Theisen W (2011) Int J Hydrogen Energy 36(17):11195
19. Olson G, Cohen M (1976) Metall Mater Trans A 7(11): 1897
20. Olson GB, Cohen M (1981) Annu Rev Mater Sci 11:1
21. Tyson W (1984) Metall Trans A-Phys Metall Mater Sci 15(7): 1475
22. Buckley JR, Hardie D (1993) Corros Sci 34(1):93
23. Mine Y, Tachibana K, Horita Z (2011) Mater Sci Eng: A 528(28):8100
24. Mine Y, Horita Z, Murakami Y (2010) Acta Mater 58:649
25. Jun JH, Choi CS (1998) Mater Sci Eng A—Struct Mater Prop Microstruct Proc 257(2):353
26. Varma SK, Kalyanam J, Murr Le, Srinivas V (1994) J Mater Sci Lett 13:107

27. Nohara K, Ono Y, Ohashi N (1977) ISIJ Int 63(5):212
28. Ulvan E, Kousaris A (1988) Metall Trans A-Phys Metall Mater Sci 19(9):2287
29. Borchers C, Michler T, Pundt A (2008) Adv Eng Mater 10:11
30. Grabke HJ (1968) Ber Bunsenges phys Chem 72: 541. doi: 10.1002/bbpc.19680720410
31. Barthelemy H (2011) Int J Hydrogen Energy 36:2750
32. Weber S, Martin M, Theisen W (2010) HTM J Heat Treatm Mat 65(4):S. 230
33. Weber S, Martin M, Theisen W (2011) Mater Sci Eng: A 528(25–26):7688